Saeed Khirkhahan [1]
Majid Jafar Tafreshi [1*]
Sanaz Alamdari [2]**
Elaheh Gharibshahian [3]

[1] Faculty of Physics,
Semnan University,
P.O. Box 35195-363,
Semnan, IRAN
* mtafreshi@semnan.ac.ir
[2] Department of Nanotechnology,
Faculty of New Sciences and Technologies,
Semnan University,
Semnan, 35131-19111, IRAN
** s.alamdari@semnan.ac.ir
[3] Department of Physics,
National University of Skills (NUS),
P. O. Box 1435761137,
Tehran, IRAN

Synthesis, Characterization, and Mechanical Properties of KTP Nanoparticles Incorporated into PMMA Matrix

This work examines the production and analysis of potassium titanium phosphate (KTP) nanoparticles that are combined with a polymethyl methacrylate (PMMA) matrix to create a KTP/PMMA nanocomposite film. KTP nanoparticles were produced using a simple hydrothermal method with oxalic acid as a coating agent. The nanocomposite films were created by dispersing KTP nanoparticles in PMMA with the use of ultrasonic energy, followed by a vacuum treatment to remove any air bubbles. Characterization tests have supported the formation of KTP nanoparticles exhibiting an orthorhombic phase, as confirmed by the structural study. The nanocomposite film showed a 38% visible transparency and an optical absorption peak at 282 nm. This indicates that the nanocomposite film had a bandgap of 4.39 eV. The resultant nanoparticles obtained by hydrothermal synthesis exhibit a relatively rhombohedral to prismatic shape with a size of 0.7–1µm. Mechanical testing revealed that the nanocomposite outperformed pure PMMA in terms of Young's modulus and tensile strength. However, the nanocomposite had a lower elongation at break, indicating its increased stiffness and strength. The results emphasize the potential of KTP/PMMA nanocomposite films in applications that need excellent optical clarity and mechanical strength.

***Keywords*:** Nanoparticles; Nanocomposites; Optical properties; KTP nanoparticles
Received: 5 November 2024; **Revised:** 21 January; **Accepted:** 28 January 2025

1. Introduction

Nanocomposite materials have gained considerable attention in recent years in scientific and technical fields due to their distinct mix of features resulting from the dispersion of nanoscale additions inside a matrix material [1-4]. A very promising research field focuses on incorporating potassium titanyl phosphate (KTP) nanoparticles into polymethyl methacrylate (PMMA) matrices to produce composite films that exhibit improved optical and mechanical properties [5,6]. KTP is widely recognized for its exceptional nonlinear optical characteristics, including second harmonic generation (SHG) and optical parametric oscillation (OPO). This makes it a highly promising option for enhancing the capabilities of optical devices and sensors [7-9]. When incorporated into a PMMA matrix, KTP nanoparticles maintain their inherent optical characteristics and also take advantage of PMMA's durability and simplicity in handling. This synergy offers a flexible and adaptable platform that may be used for a wide range of applications, including photonics, biophotonics, improved coatings, and flexible electronics [10-12]. The advancement of KTP/PMMA nanocomposite films has considerable potential for many reasons. The addition of KTP nanoparticles improves the optical characteristics of PMMA films, allowing for their use in nonlinear optics applications, such as frequency doubling and signal processing [13]. PMMA enhances the mechanical strength and endurance of the composite, which is essential for applications that need both structural integrity and optical functioning. PMMA's exceptional processability enables the easy integration and even distribution of KTP nanoparticles, making it possible to create intricate structures and devices. This technology may be applied in a wide range of disciplines, including as telecommunications, biological sensing, solar energy conversion, and flexible electronics [14-17]. It is particularly important in these fields to have materials that are both optically clear and mechanically strong. The synthesis method and the capping agent significantly influence the features of nanoparticles, both optical and structural [18-27]. Synthesis methods like chemical reduction, sol-gel, and hydrothermal can make nanoparticles of different sizes, shapes, and crystallinities. These processes can modify optical properties like absorption, emission, and scattering [28]. Choosing the right capping agent affects the surface chemistry and optical properties of the nanoparticles, which in turn controls how stable they stay and stops them from sticking together. The presence of capping agents can also impact the structural integrity and surface morphology of nanoparticles, influencing their functional properties and potential applications in fields such as biomedicine, electronics, and photonics [29]. In a recent study a composite of KTP nanoparticles (~400 nm) wrapped in 3D reduced graphene oxide (rGO) was prepared [30]. The synergy between the 3D carbon networks and KTP results in excellent properties. When used as an anode for potassium-ion batteries (KIBs), the composite demonstrates outstanding electrochemical

performance. In another study a free-standing film of $KTi_2(PO_4)_3$ nanoparticles encapsulated in porous N-doped carbon nanofibers was fabricated using electrospinning technology [31]. The highly conductive N-doped carbon matrix enhances intrinsic electronic conductivity and accelerates ion diffusion kinetics. This electrode showed remarkable electrochemical performance in both sodium-ion and potassium-ion batteries. Bi_2Te_3 nanosheets were synthesized via ultrasound-assisted exfoliation and used as a saturable absorber (SA) in a Q-switched mode-locked (QML) laser [32]. This setup successfully generated sub-nanosecond pulses in a KTP-based intracavity optical parametric oscillator (IOPO) with a minimum pulse duration of 520 ps at 2 kHz. This is the first use of Bi_2Te_3 SA in a solid-state QML IOPO laser, demonstrating its potential for generating sub-nanosecond pulses. Simulations of coupled rate equations matched experimental results, showing Bi_2Te_3 promise for optoelectronic applications. Overall, the continuous progress in semiconductor/KTP/PMMA nanocomposite films highlights their crucial contribution to the evolution of optical technologies and materials research [33,34].

This article seeks to investigate the creation, characteristics, and uses of these groundbreaking substances, emphasizing their revolutionary influence in several technical fields.

2. Experimental Work

Deionized water, tetrabutylammonium hydroxide, potassium dihydrogenphosphate, chloroform, potassium carbonate, oxalic acid were employed as raw materials. To produce potassium titanyl phosphate ($KTiOPO_4$) nanocrystals, hydrothermal method was used. A titanium solution was created by combining a 1 M stoichiometric ratio of Tetrabutylammonium hydroxide, with 40 mL of deionized (DI) water. Subsequently, a solution containing potassium dihydrogen phosphate was added to the mixture at a molar ratio of 1:1 Ti^{4+}. The resulting mixture was then vigorously stirred until it achieved homogeneity. Produced solution was transported into an autoclave, tightly sealed, and subjected to heating in a preheated oven at a temperature of 170 °C for a duration of 48 hours. Following the heating process, the autoclave was left to undergo natural cooling until it reached the ambient temperature of the room. The final product was subjected to several washes with distilled water to eliminate contaminants, followed by drying at a temperature of 100 °C. The desiccated substance was further pulverized into fine particulates using a mortar and pestle, and these particulates were subjected to annealing at a temperature of 700 °C for a duration of 2 hours. 1 wt.% of KTP nanoparticles was used to make KTP nanocomposite with polymer matrix (PMMA). A vacuum step was used to eliminate air bubbles after the mixture had been dispersed using ultrasonic energy for 30 min. The mixture was dropped on petri dish and dried. Finally, flexible composite films were formed. Figure (1) displays the created composite image.

The x-ray diffraction (XRD) analysis was conducted on the materials using an Advanced Bruker D8 X-ray diffractometer with CuKα radiation (λ=1.5405Å). XRD patterns were used to calculate the grain size, lattice strain, and structural phase of KTP nanoparticles. The KBr pellet approach was used to record Fourier-transform infrared (FTIR) spectra using an 8400S-SHIMADZU infrared spectrometer in the range of 400-4000 cm^{-1}. This investigation examined the structural development of KTP nanoparticles. Nanoparticle morphology was recorded using a HITACHI S4160 scanning electron microscope. Mechanical parameters were measured using a Stable Micro Systems texture analyzer in accordance with industry standards (ASTM D-882-97).

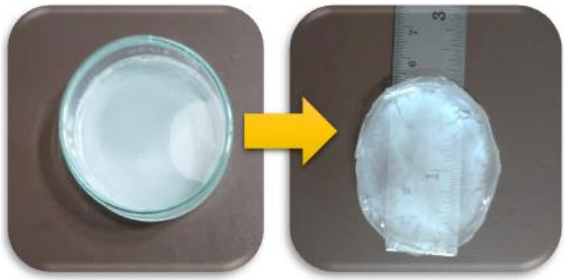

Fig. (1) Photographs of the prepared nanocomposite

3. Results and Discussion

Figure (2) shows the XRD patterns of synthesized KTP nanoparticles, neat polymer, and prepared nanocomposite. All patterns confirm the formation of $KTiOPO_4$ nanoparticles with an orthorhombic phase (standard ASTM card 01-080-0893). Figure (2b) shows the PMMA's characteristic peaks at 15° and 30°. These two characteristic peaks can be clearly seen in Fig. (2c) along with the characteristic peaks of KTP, and it confirms the formation of the KTP polymer nanocomposite structure. The constants of the crystal lattice, the grain size of the obtained nanoparticles, and the strain on the crystal lattice for KTP nanoparticle without the oxalic acid coating agent and with the use coating agent in each method are given in table (1).

Table (1) XRD parameters of the synthesized KTP NPs

Sample	Crystallite Size (nm)	Strain (ε)	Unit Cell Parameters (Å)		
			a	b	c
Synthesized KTP NPs	43.51	0.0036	12.81	6.39	10.58

UV–visible spectroscopy is a technique used to measure the light transmittance of a sample in the UV-visible range of the electromagnetic spectrum. Figure (3) presents the UV-visible absorption and transmission spectra of the prepared sample. The bandgap of the

generated KTP nanoparticles was determined using the following equation [35]:

$$E_g = \frac{h\nu}{\lambda_{onset}} \approx \frac{1240}{\lambda_{onset}} \quad (1)$$

The value of λ_{onset} was determined by extrapolating the absorption edge onto the wavelength axis. Prepared nanocomposite sample has 38% transparency in the visible region and a significant optical absorption at the wavelength of 282 nm with the energy band gap of 4.39 eV.

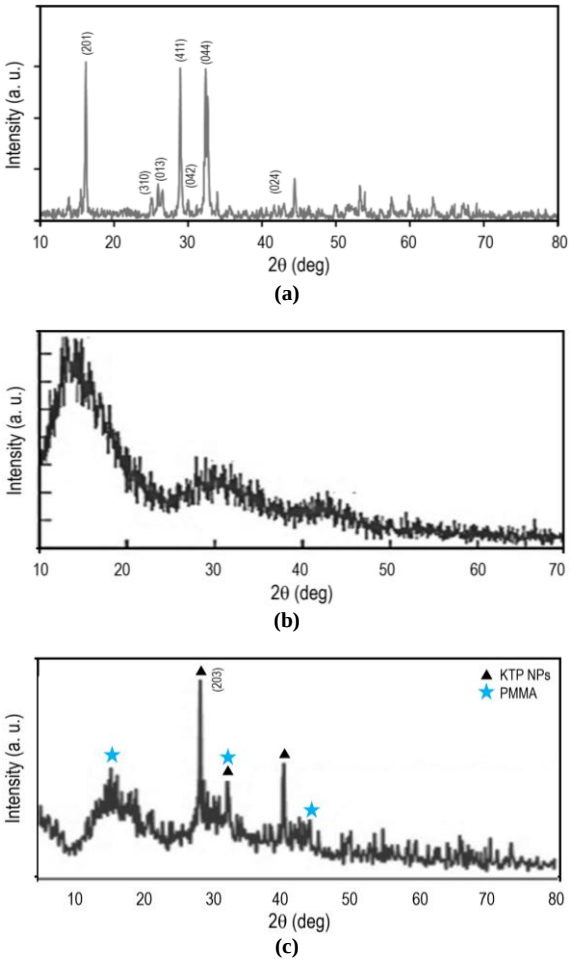

Fig. (2) XRD patterns of (a) synthesized KTP nanoparticles, (b) PMMA, and (c) prepared nanocomposite

The FTIR spectra of KTP nanoparticles prepared by the hydrothermal method are shown in Fig. (4). These nanoparticles are mixed with a coating agent and polymer in a 1:1 molar ratio to make a polymer matrix (PMMA). The obtained spectrum clearly displays the characteristic peaks of KTP and PMMA, confirming the formation of the nanocomposite structure. It is observed that KTP characteristic links in the range of 600-1200 cm^{-1}. Six bonds at 974, 995, 1027, 1050, 1100, and 1126 cm^{-1} belong to the v_3 asymmetric tensile bonds of the PO_4 group [19]. In the deformed octahedral structure of TiO_6, three bonds located at 712, 785, and 820 cm^{-1} correspond to Ti-O vibrations. The v_2 and v_4 modes in the PO_4 group are responsible for the remaining peaks in the 350-660 cm^{-1} range [18,19].

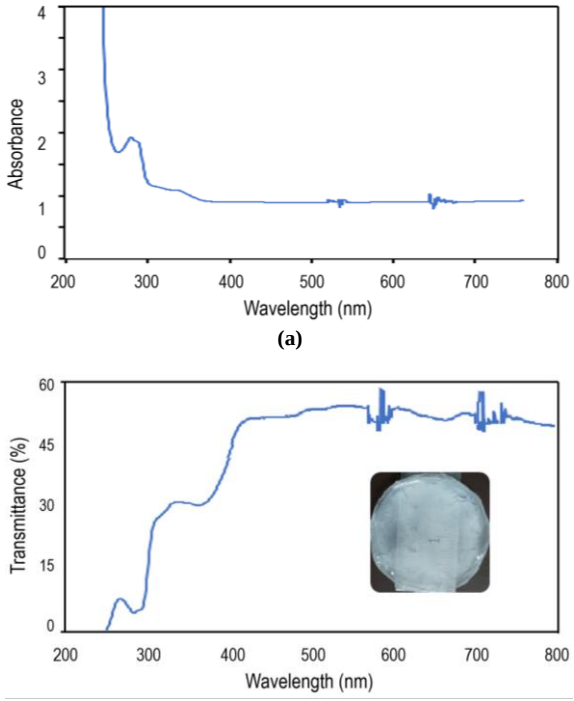

Fig. (3) UV-visible absorption (a) and transmission (b) spectra of the prepared nanocomposite

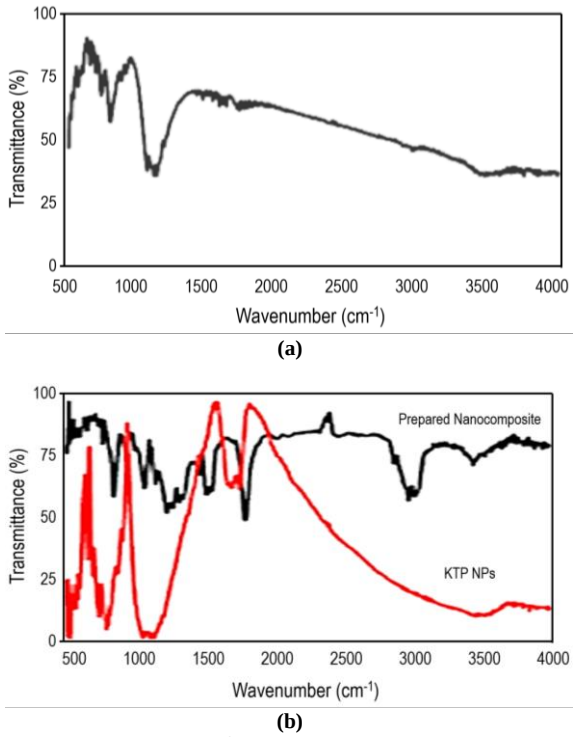

Fig. (4) FTIR spectra of (a) KTP NPs, and (b) the prepared nanocomposite samples

Figure (5) shows the field-emission scanning electron microscope (FE-SEM) images of the synthesized KTP powders and the surface of the

prepared KTP/PMMA nanocomposite. The structure of the particles appears to be dense and agglomerated, with irregular shapes and relatively large particle at a higher magnification more details of the KTP powder's structure are revealed. Smaller particles with relatively sharp edges are visible.

The surface of the KTP/PMMA nanocomposite in Fig. (5c) is smooth and has a little aggregation of nanoparticles. The nanoparticles produced by hydrothermal synthesis relatively exhibiting a rhombohedral to prismatic shape with a size of 0.7–1 μm.

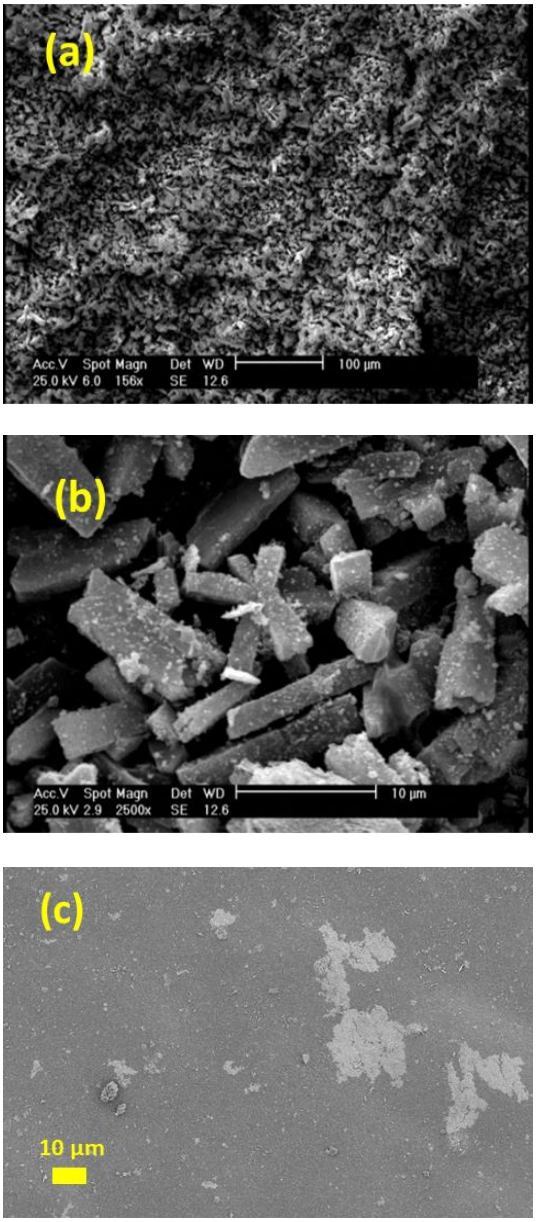

Fig. (5) FE-SEM images (a,b) of synthesized KTP powders, and (c) of the surface of the prepared KTP/PMMA nanocomposite

Table (2) displays the mechanical properties of the pure PMMA and composite samples that were manufactured. The nanocomposite exhibits a higher Young's Modulus and tensile strength compared to pure PMMA, indicating increased stiffness and enhanced adhesion from KTP nanoparticles. The nanocomposite also demonstrates reduced elongation at fracture, suggesting lower deformability due to enhanced rigidity. While the nanocomposite offers greater rigidity and durability, its reduced malleability may limit applications requiring high pliability. The inclusion of KTP nanoparticles in PMMA composites has potential applications in sectors requiring a combination of optical, mechanical, and possibly electrical properties. The incorporation of KTP nanoparticles into a composite film made of PMMA has potential uses in several sectors, especially in situations where the combination of optical, mechanical, and perhaps electrical characteristics is beneficial.

Table (2) Mechanical properties of the prepared samples

Sample	Young's Modulus (MPA)	Tensile Strength (MPA)	Elongation at Break (%)
Neat PMMA	2750	65	3.5
Prepared Nanocomposite	3200	70	2

4. Conclusion

This study demonstrated the successful integration of KTP nanoparticles into a PMMA matrix via hydrothermal synthesis and nanocomposite film fabrication. The orthorhombic phase of KTP was confirmed, while the presence of both KTP and PMMA in the composite was validated. A strong optical absorption edge at 282 nm was revealed, corresponding to a bandgap of 4.39 eV, highlighting its potential for optical applications. Mechanical testing showed enhanced rigidity and strength compared to neat PMMA, though flexibility was reduced due to lower elongation at break. The nanoparticles exhibited rhombohedral to prismatic shapes with sizes of 0.7–1 μm. These findings suggest that KTP/PMMA nanocomposites hold promise for optical technologies, coatings, and flexible electronics. Future work should focus on optimizing nanoparticle dispersion to further improve their properties.

Acknowledgements

The authors acknowledge the Semnan University and SHAHAB Parto Negar (Radonik) Company for providing characterization facilities.

References

[1] A. Kathalingam et al., "Characterization and application of flexible, highly conductive freestanding films of SWCNT and PMMA nanocomposite prepared by facile solution method", *Surf. Interfaces*, 40 (2023) 103161.

[2] H. Chathuranga et al., "Preparation of bioinspired graphene oxide/PMMA nanocomposite with improved mechanical properties", *Compos. Sci. Technol.*, 216 (2021) 109046.
[3] F.J. Kadhim et al., "Photocatalytic activity of TiO_2/SiO_2 nanocomposites synthesized by reactive magnetron sputtering technique", *J. Nanophot.*, 16(2) (2022) 026005.
[4] M.K. Ali and F.J. Kadhim, "Structural Characteristics of TiO_2/TiN Nanocomposites Synthesized by DC Reactive Magnetron Sputtering Technique", *Iraqi J. Appl. Phys.*, 19(3A) (2023) 49-54.
[5] H. Lv et al., "Properties of Rubidium-Doped Potassium Titanyl Phosphate (Rb:KTP) Grown by Hydrothermal Method", *J. Phys.: Conf. Ser.*, 2679 (2024) 012025.
[6] D. Li et al., "Solution-processable three-dimensionally macroporous $KTiOPO_4/SiO_2$ inverse opal powders with enhanced second harmonic emission", *J. Alloys Comp.*, 746 (2018) 256-261.
[7] S.P. Singh, S.K. Sharma and D.Y. Kim, "Carrier mechanism of ZnO nanoparticles-embedded PMMA nanocomposite organic bistable memory device", *Solid State Sci.*, 99 (2020) 106046.
[8] A.K. Yousef et al., "Analytical Investigation for the Effect of Carrier Concentration and Temperature on the Nonlinear Properties of the Semiconductor Lasers Operating at Near - Infrared Wavelengths", *Eng. Technol. J.*, 24(4) (2005) 147-159.
[9] O.A. Hammadi and M.S. Edan, "Temperature Dependencies of Refractive Index and Optical Elasticity Coefficient on Lens Induced in Nd:YAG Crystal", *Iraqi J. Appl. Phys.*, 8(1) (2012) 35-41.
[10] A. Marimuthu, R.N. Perumal and S. Gaur, "Investigations on dielectric and ferroelectric properties of molybdenum doped potassium titanyl phosphate single crystal ($KTiOPO_4$)", *Mater. Sci. Eng. B*, 288 (2023) 116185.
[11] S. Neufeld et al., "Vibrational Properties of the Potassium Titanyl Phosphate Crystal Family", *Crystals*, 13 (2023) 1423.
[12] L. Mentasti et al., "Facile functionalization of $YVO_4:Eu^{3+}$: From nanoparticles to luminescent PMMA nanocomposites for radiation detectors", *Opt. Mater.*, 129 (2022) 112566.
[13] E. Gharibshahian et al., "The effect of capping agent on morphology, surface functionalization, and bio-compatibility properties of $KTiOPO_4$ nanoparticles", *Heliyon*, 10(23) (2024) e40513.
[14] F. Lin et al., "Morphological and mechanical properties of graphene-reinforced PMMA nanocomposites using a multiscale analysis", *Comput. Mater. Sci.*, 150 (2018) 107-120.
[15] F. Ye et al., "Self-assembled nanofibrillar gel network toughened PMMA nanocomposite by in situ thermal polymerization of MMA gel", *Colloids Surf. A: Physicochem. Eng. Asp.*, 480 (2015) 1-10.
[16] M.S. Rise et al., "Synthesis and characterization of ZnO nanorods-Zn_2SiO_4 nanoparticles-PMMA nanocomposites for UV-C protection", *Opt. Mater.*, 123 (2022) 111922.
[17] P. Jain et al., "Comparative analysis of machine learning techniques for predicting wear and friction properties of MWCNT reinforced PMMA nanocomposites", *Ain Shams Eng. J.*, 15(9) (2024) 102895.
[18] E. Gharibshahian, M.J. Tafreshi and M. Behzad, "The effects of solution pH on structural, optical and electrical properties of $KTiOPO_4$ (KTP) nanoparticles synthesized by hydrothermal method", *Opt. Mater.*, 109 (2020) 110230.
[19] E. Gharibshahian et al., "Theoretical and experimental investigation of the effect of acetic and formic acids as capping agents on morphology of $KTiOPO_4$ nanoparticles", *Nanochem. Res.*, 8 (2023) 181-189.
[20] E. Gharibshahian and M.J. Tafreshi, "The effect of cooling rate on size, quality and morphology of $KTiOPO_4$ (KTP) crystals grown by different nucleation techniques", *Cryst. Res. Technol.*, 50 (2015) 603-612.
[21] S. Alamdari, M.H.M Ara and M.J. Tafreshi, "Synthesize and optical response of ZnO/$CdWO_4$:Ce nanocomposite with high sensitivity detection of ionizing radiations", *Opt. Laser Technol.*, 151 (2022) 107990.
[22] M. Hosseinpour et al., "Development of a novel flexible thin PWO(Er)/ZnO(Ag) nanocomposite for ionizing radiation sensing", *J. Alloys Comp.*, 967 (2023) 171678.
[23] P. Vatani, M. Aliannezhadi and F.S Tehrani, "Improvement of optical and structural properties of ZIF-8 by producing multifunctional Zn/Co bimetallic ZIFs for wastewater treatment from copper ions and dye", *Sci. Rep.*, 14 (2024) 15434.
[24] H. Farhadi et al., "One-step hydrothermal synthesis of $CeVO_4$/bentonite nanocomposite as a dual-functional photocatalytic adsorbent for the removal of methylene blue from aqueous solutions", *Sci. Rep.*, 14 (2024) 14824.
[25] S. Azadmehr et al., "Substrate and Cu concentration-dependent physical properties of spray-deposited Cu_2ZnSnS_4 thin films: a comparative study", *J. Mater. Sci.: Mater. Electron.*, 35 (2024) 855.
[26] S. Alamdari et al., "Flexible mixed oxides thin films: zinc oxide/cadmium tungstate/chitosan for optical devices", *Opt. Quantum Electron.*, 56 (2024) 443.
[27] S. Alamdari et al., "Erbium doped Barium Tungstate-Chitosan Nanocomposite: Luminescent

Properties", *Prog. Phys. Appl. Mater.*, 3 (2023) 119-123.

[28] S. Tabanli and G. Eryurek, "Upconversion luminescence properties of Y_2O_3:Yb^{3+}/Er^{3+}/Tm^{3+} nanocrystal doped PMMA nanocomposites", *J. Non-Cryst. Solids*, 505 (2019) 43-51.

[29] W. Cai et al., "Preparation and luminescent properties of GdOF:Ce, Tb nanoparticles and their transparent PMMA nanocomposites", *Opt. Mater.*, 43 (2015) 36-41.

[30] S. Huang and G. Xu., "$KTi_2(PO_4)_3$ nanoparticles wrapped in 3D RGO as enhanced electrode for potassium-ion batteries", *Mater. Lett.*, 361 (2024) 136156.

[31] J. Dong et al., "Encapsulation of $KTi_2(PO_4)_3$ nanoparticles in porous N-doped carbon nanofibers as a free-standing electrode for superior Na/K-storage performance", *J. Alloys Comp.*, 937 (2023) 168358.

[32] C. Han et al., "Sub-nanosecond single mode-locking pulse generation in an intracavity KTP optical parametric oscillator with a few-layer Bi_2Te_3 topological insulator saturable absorber", *Infrared Phys. Technol.*, 139 (2024) 105302.

[33] M Banari et al., "CeO_2:ZnO hybrid nanorods for self-powered UV-photodetectors", *Ceram. Int.*, 51 (2025) 9-16.

[34] M.I Al-Shemri et al., "Au-$H_2Ti_3O_7$ nanotubes for non-invasive anticancer treatment by simultaneous photothermal and photodynamic therapy", *Sci. Rep.*, 14 (2024) 25998.

[35] C. Kittel, "**Introduction to Solid State Physics**", 8th ed., John Wiley & Sons, Inc. (2005) p. 276.

